Quantitative Structure−Activity Relationship Analysis of Inhibitors of the Nicotine Metabolizing CYP2A6 Enzyme

Minna Rahnasto,[†] Hannu Raunio,[†] Antti Poso,[‡] Carsten Wittekindt,[‡] and Risto O. Juvonen*,[†]

Department of Pharmacology and Toxicology, University of Kuopio, POB 1627, 70211 Kuopio, Finland, and Department of Pharmaceutical Chemistry, University of Kuopio, POB 1627, 70211 Kuopio, Finland

Received June 14, 2004

The purpose of this study was to develop screening and in silico modeling methods to obtain accurate information on the active center of CYP2A6, a nicotine oxidizing enzyme. The inhibitory potencies of 26 naphthalene and 16 non-naphthalene derivatives were determined for human CYP2A6 and mouse CYP2A5 enzymes. Several comparative molecular field analysis (CoMFA) models were developed to find out what types of steric and electrostatic properties are required for potent inhibitors. The IC_{50} values of the tested compounds varied from 0.55 to 35 400 μM for CYP2A6 and from 1 to 1500 μM for CYP2A5. The generated CoMFA models were able to accurately predict the inhibition potencies of an external test set of chemicals. Potent and specific inhibitors of the CYP2A6 enzyme can be used in the future to increase nicotine bioavailability and thus make oral nicotine administration feasible in smoking cessation therapy.

Introduction

Tobacco is an insidious chemical package because among its numerous toxic, mutagenic, and carcinogenic compounds it contains nicotine, which is responsible for causing the dependency associated with tobacco smoking.[1] According to the World Health Organization (WHO), tobacco use is the leading cause of the disease burden measured in disability adjusted life years in developed countries and one of the top 10 health risk factors even in the poorest developing regions.[2,3]

Nicotine is the essential component smokers seek from tobacco use. Various nicotine preparations have been developed as medication to assist in smoking cessation, and nicotine has also been evaluated in the treatment of a variety of medical disorders.[4] After entering the circulation, active nicotine is eliminated mainly by metabolism to cotinine. The main enzymes catalyzing this reaction are cytochrome P450 2A6 (CYP2A6) and aldehyde oxidase with CYP2A6 being the rate-limiting enzyme.[5−7] Individuals having deficient CYP2A6 enzyme function, due to inactive alleles of the CYP2A6 gene, display a decreased capacity for nicotine metabolism, and these individuals may be less likely to become smokers.[8−11] Pilot studies show that chemical inhibition of the CYP2A6 enzyme can reduce smoking frequency.[11,12]

In addition to nicotine, the human CYP2A6 and mouse cytochrome P450 2A5 (CYP2A5) enzymes metabolize several other xenobiotics, such as many tobacco-specific nitrosamines and other toxic compounds.[5,6,13] Recent experimental evidence shows that chemical inhibition of the CYP2A enzyme in the mouse dramatically reduces lung tumorigenesis caused by a highly carcinogenic nitrosamine.[14] There is evidence that, especially in the Japanese population, individuals with inactive CYP2A6 alleles are protected from developing lung cancer caused by cigarette smoking.[10,15]

Nicotine is routinely used in smoking cessation therapy. Nicotine is currently administered as chewing gum, as transdermal patches, or via inhalation. Oral nicotine administration is not possible because of the very high degree of CYP2A6 mediated first pass metabolism in the liver. Because oxidation by CYP2A6 is the rate-limiting step in nicotine inactivation, blocking this reaction by a chemical inhibitor would increase nicotine bioavailability and allow for oral administration of nicotine.[7]

Today, there is enough data available on CYP2A inhibitors to establish crude structure−activity relationships because approximately 200 compounds have been tested for their inhibitory properties on CYP2A5 or CYP2A6.[16−20] We have previously carried out quantitative structure−activity relationship (QSAR) analysis of inhibitors of the CYP2A5 and CYP2A6 enzymes using the comparative molecular field analysis (CoMFA) method.[21,22] Comparative modeling of CYP2A6 has shown that inhibitors of the CYP2A enzymes are generally planar molecules with two hydrogen bond acceptors.[23] The results of these studies have yielded structural information of substrate and inhibitor interactions with the CYP2A5 and CYP2A6 enzymes, but further refinement of these models is needed.[16,22]

The main purpose of this study was to elucidate the inhibitory structure−activity relationships of CYP2A6 and CYP2A5 enzymes in finer detail, with the ultimate aim of predicting and developing a potent and specific inhibitor of CYP2A6. A series of naphthalene derivatives were used because naphthalene, which is structurally close to coumarin (Figure 1), is a relatively potent inhibitor of both enzymes.[24] The inhibitory potencies of 26 naphthalene derivatives and 16 non-naphthalene compounds were determined, and the values obtained in CYP2A6 and CYP2A5 were compared. Several CoMFA models were developed to find out which

* Author for correspondence. Telephone: 358-17-162010. Fax: 358-17-162424. E-mail: Risto.Juvonen@uku.fi.
[†] Department of Pharmacology and Toxicology.
[‡] Department of Pharmaceutical Chemistry.

10.1021/jm049536b CCC: $30.25
Published on Web 12/24/2004

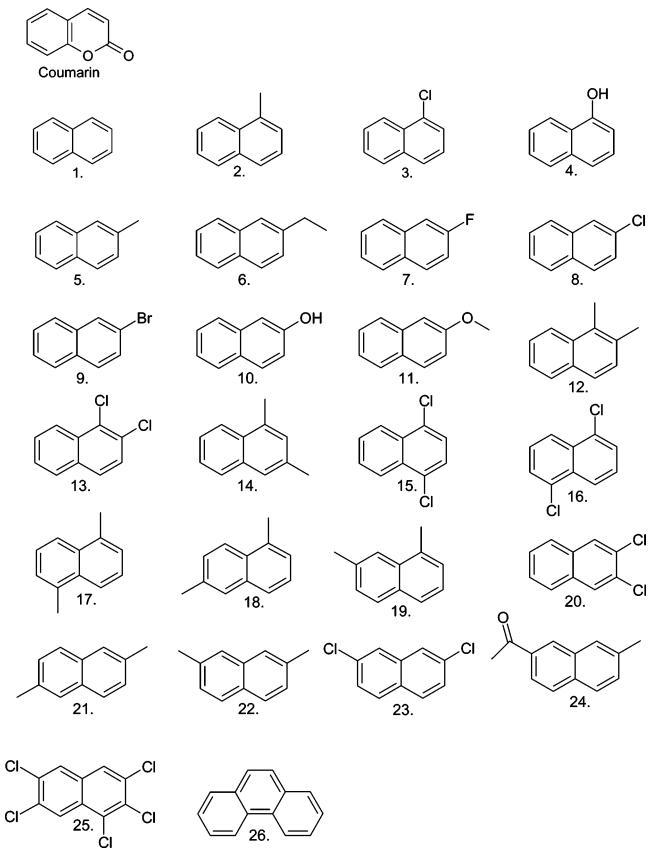

Figure 1. Structures of the naphthalene derivatives.

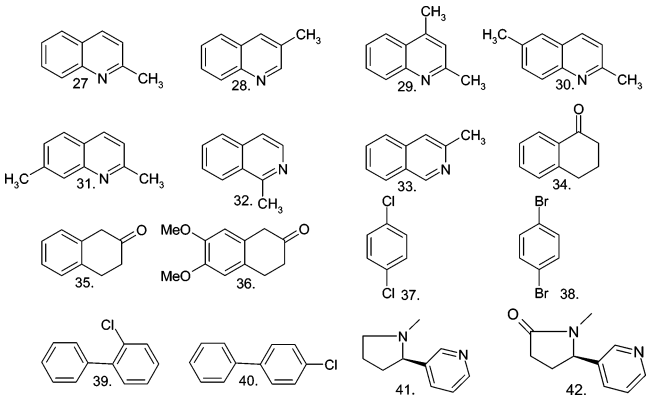

Figure 2. Structures of the non-naphthalene derivatives.

structural features are important for the inhibition potency of these compounds.

Results

Inhibition of CYP2A6. The inhibitory potencies of a series of derivatives of naphthalene ($n = 26$), quinoline ($n = 7$), tetralone ($n = 3$), and six non-planar compounds (Figures 1 and 2) were tested toward both CYP2A6 and CYP2A5 enzymes. For CYP2A6, the lowest IC_{50} values (<1 μM) were obtained with 2-bromonaphthalene and 2-fluoronaphthalene, whereas cotinine gave the highest value (35 000 μM) (Table 1). The IC_{50} values of 11 naphthalene derivatives were lower than that of naphthalene. Fluoro, chloro, bromo, methyl, and ethyl substitutions at position 2 of naphthalene decreased the IC_{50} value. Also, for example, 2,7-dimethyl, 1,3-dimethyl, and 2,6-dimethyl as well as 1,3-dichloro and 1,5-dichloro substitutions of naphthalene inhibited CYP2A6 more potently than naphthalene. The IC_{50} values of all quinoline and isoquinoline derivatives were higher than those of their corresponding naphthalene derivatives, indicating that a heterocyclic nitrogen atom decreases the inhibition potency. Also, the IC_{50} values of the xylol derivatives as well as nicotine and cotinine were high (Table 1).

Inhibition of CYP2A5. The IC_{50} values for CYP2A5 ranged from 1.0 μM (dichloro-*p*-xylol) to 1500 μM (cotinine) (Table 2). 1,2,3,6,7-Pentachloronaphthalene, 1-naphthol, and 2-naphthol inhibited CYP2A5 less potently than naphthalene. All of the other naphthalene derivatives tested exhibited greater inhibition potencies than the parent compound. Several similar structure−activity relationship trends as for CYP2A6 were observed. The substitution of fluoro, chloro, bromo, methyl, or ethyl at position 2 of naphthalene as well as chloro/methyl disubstitution decreased the IC_{50} values. Most quinoline and isoquinoline derivatives increased the IC_{50} values compared with the corresponding naphthalene derivatives. However, there were also some pronounced differences between CYP2A5 and CYP2A6 enzymes. For example, dibromo-*p*-xylol, dichloro-*p*-xylol, and 2-dichloronaphthalene inhibited potently CYP2A5 but not CYP2A6.

CYP2A6/CYP2A5 Comparison. Human CYP2A6 to mouse CYP2A5 IC_{50} ratio of inhibitors were calculated for each compound (Table 3).[16] Seven compounds, for example, 2-halogen naphthalenes, naphthalene, and 1-methylisoquinoline, belonged to the first group, in which this ratio is less than 0.67, indicating that these compounds were more potent inhibitors of CYP2A6 than CYP2A5. Nine compounds, for example, 1,3-dimethylnaphthalene, in the second group inhibited these enzymes equally, their CYP2A6/CYP2A5 ratio being between 0.67 and 1.49. Most of the compounds tested fell into the third group in which the CYP2A6/CYP2A5 ratio was higher than 1.49, indicative of more potent inhibition of CYP2A5 than of CYP2A6. The IC_{50} values of 2-methoxynaphthalene, 2,7-dichloronaphthalene, dichloro-*p*-xylol, dibromo-*p*-xylol, and cotinine were at least 10 times lower for CYP2A5 than those for CYP2A6.

CoMFA Models. Two standard CoMFA models for CYP2A6, one standard CoMFA model for CYP2A5 using steric and electrostatic fields alone, and one CYP2A6 model with the lowest unoccupied molecular orbital (LUMO) fields were created to elucidate detailed QSARs of the studied molecules. The obtained statistics of the models are summarized in Table 4. All models gave q^2 values of at least 0.5 with 3−4 partial-least-squares (PLS) components.

CoMFA contour maps were generated from all CYP2A6 and CYP2A5 CoMFA models. The CYP2A6 model with the LUMO fields (model III) was statistically the most significant (Figure 5). Also, the CYP2A5 model (model IV) is represented as a 3D contour map (Figure 6). In these maps, the colored regions indicate steric and electrostatic interactions that are associated with inhibition potencies. Areas where increased steric interaction is correlated with higher inhibition potency are marked in green. Regions where the presence of bulk decreased the inhibition potency are colored in yellow. Red regions indicate areas where an increase in elec-

Table 1. Inhibition of CYP2A6 by Naphthalene and Non-naphthalene Compounds[a]

compound no.[b]	naphthalene derivatives	IC_{50} (μM)	95% confidence intervals	superposition group[c]
9	2-bromonaphthalene	0.55	(0.38−0.72)	1
7	2-fluoronaphthalene	0.67	(0.28−1.1)	1
22	2,7-dimethylnaphthalene	1.7	(1.1−2.2)	1
5	2-methylnaphthalene	2.4	(1.9−2.8)	1
15	1,4-dichloronaphthalene	2.5	(2.1−2.8)	1
16	1,5-dichloronaphthalene	2.5	(1.6−3.5)	1
8	2-chloronaphthalene	5.4	(4.6−6.2)	1
24	7-methyl-2-naphthaldehyde	6.7	(0.5−12.9)	1
14	1,3-dimethylnaphthalene	8.3	(1.5−16)	2
21	2,6-dimethylnaphthalene	10	(5.2−15)	2
6	2-ethylnaphthalene	12	(9.0−14)	2
13	1,2-dicloronaphthalene	15	(13−17)	3
3	1-chloronaphthalene	18	(13−23)	3
1	naphthalene	25	(21−30)	2
12	1,2-dimethylnaphthalene	26	(16−36)	3
17	1,5-dimethylnaphthalene	31	(19−43)	2
19	1,7-dimethylnaphthalene	31	(22−39)	2
2	1-methylnaphthalene	34	(22−47)	2
20	2,3-dichloronaphthalene	>60		5
11	2-methoxynaphthalene	62	(24−99)	4
26	phenanthrene	97	(68−126)	5
23	2,7-dichloronaphthalene	>100		5
18	1,6-dimethylnaphthalene	130	(71−180)	5
4	1-naphthol	130	(89−171)	4
10	2-naphthol	140	(88−180)	4
25	1,2,3,6,7-pentacloronaphthalene	>600		6

compound no.[b]	others	IC_{50} (μM)	95% confidence intervals	superposition group[c]
37	dichloro-*p*-xylol	17	(11−22)	3
35	β-tetralone	21	(18−24)	3
33	3-methylisoquinoline	25	(21−29)	3
39	2-chlorobiphenyl	36	(17−54)	4
34	α-tetralone	52	(33−71)	4
38	dibromo-*p*-xylol	59	(35−83)	5
32	1-methylisoquinoline	60	(51−70)	4
40	4-chlorobiphenyl	150		5
27	quinaldine	190	(170−220)	6
28	3-methylquinoline	200	(160−240)	6
30	2,6-dimethylquinoline	280	(260−310)	6
31	2,7-dimethylquinoline	400	(330−460)	6
41	nicotine	580	(440−720)	7
29	2,4-dimethylquinoline	830	(390−1300)	6
36	6,7-dimethoxy-2-tetralone	2000		7
42	cotinine	35 000	(13 000−58 000)	7

[a] The compounds are listed in ascending order of the IC_{50} values. [b] In Figures 1 and 2. [c] Derived from superimposition of molecules.

tronegativity can enhance the inhibition potency and blue regions where electronegativity decreases its inhibition potency.

In the CYP2A6 model (model III), negative charge favored areas were near positions 2 and 4 of the naphthalene ring, indicating that a partial negative charge here will increase the inhibition potency. Similar areas were present also next to positions 5 and 7. Negative charge disfavored areas were present near position 8, and the sterically favored area near position 2 was broader than that in the CYP2A5 model. Major LUMO fields of CYP2A6 model are located near the C−C double bonds of the aromatic ring (Figure 7). In the CYP2A5 model (model IV), negative charge favored (red) areas were present around substitution at position 2 and next to position 5 of the naphthalene ring. Negative charge disfavored (blue) areas were found beside position 8 of naphthalene. The sterically favored green area was located around substitution at position 2 in the CYP2A5 model.

To assess the validity of the models, the CYP2A6 CoMFA model with MOPAC charges (model II) and the CYP2A5 CoMFA model with Gasteiger−Hückel charges (model IV) were used to predict the pIC_{50} values for an external test set of compounds (Figure 4). As summarized in Table 5, these analyses predicted well pIC_{50} values of benzaldehyde and amphetamine derivatives. The predicted pIC_{50} values in the CYP2A6 model for 4-methylbenzaldehyde, 4-methoxybenzaldehyde, amphetamine, and 2-phenylethylamine were less than 0.1 log units deviant from the experimental pIC_{50} values. The predicted IC_{50} values for benzaldehyde and 2-(*p*-tolyl)-ethylamine were within 0.1−0.25 log units of the experimental pIC_{50} values. The predicted pIC_{50} values in the CYP2A5 model for four compounds were within 0.5−1.0 log units of the experimental pIC_{50} values. Predictions for amphetamine and 2-phenylethylamine yielded pIC_{50} values that were more than 1.0 log units of the experimental pIC_{50} values.

Discussion

The principal aim of this study was to determine new molecular properties affecting the interaction between a chemical inhibitor and the human CYP2A6 enzyme.

Table 2. Inhibition of CYP2A5 by Naphthalene and Non-Naphthalene Compounds[a]

compound no.[b]	naphthalene derivatives	IC_{50} (μM)	95% confidence intervals	superposition group[c]
22	2,7-dimethylnaphthalene	1.4	(0.98−1.9)	1
21	2,6-dimethylnaphthalene	1.7	(1.5−2.1)	1
16	1,5-dichloronaphthalene	2.4	(1.5−3.3)	1
9	2-bromonaphthalene	2.5	(1.9−5.9)	1
24	7-methyl-2-naphthaldehyde	4.1	(2.8−5.4)	1
23	2,7-dichloronaphthalene	4.4	(3.3−5.5)	1
11	2-methoxynaphthalene	4.6	(2.3−6.7)	1
6	2-ethylnaphthalene	4.8	(3.5−6.1)	1
13	1,2-dicloronaphthalene	5.5	(3.5−7.5)	2
15	1,4-dichloronaphthalene	5.5	(3.5−7.5)	2
5	2-methylnaphthalene	7.0	(4.9−9.1)	2
7	2-fluoronaphthalene	7.3	(1.3−13)	2
14	1,3-dimethylnaphthalene	9.9	(3.6−16)	2
8	2-chloronaphthalene	12	(10−15)	2
3	1-chloronaphthalene	14	(11−17)	2
19	1,7-dimethylnaphthalene	14	(9.0−18)	2
12	1,2-dimethylnaphthalene	24	(17−31)	2
2	1-methylnaphthalene	24	(14−35)	2
26	phenanthrene	26	(17−34)	2
18	1,6-dimethylnaphthalene	32	(22−41)	2
17	1,5-dimethylnaphthalene	34	(25−42)	2
20	2,3-dichloronaphthalene	60		3
1	naphthalene	74	(65−83)	3
10	2-naphthol	78	(54−100)	3
4	1-naphthol	140	(86−190)	3
25	1,2,3,6,7-pentacloronaphthalene	300		3

compound no.[b]	others	IC_{50} (μM)	95% confidence intervals	superposition group[c]
37	dichloro-*p*-xylol	1.0	(0.68−1.4)	1
38	dibromo-*p*-xylol	2.2	(1.7−2.7)	1
33	3-methylisoquinoline	4.8	(26−29)	1
35	β-tetralone	9.7	(7.8−12)	2
39	2-chlorobiphenyl	13	(7−17)	2
34	α-tetralone	14	(13−16)	2
40	4-chlorobiphenyl	18	(8.6−28)	2
30	2,6-dimethylquinoline	40	(33−48)	3
27	quinaldine	80	(73−87)	3
28	3-methylquinoline	100	(86−120)	3
29	2,4-dimethylquinoline	110	(89−130)	3
41	nicotine	160	(88−220)	4
32	1-methylisoquinoline	170	(150−180)	3
31	2,7-dimethylquinoline	180	(160−210)	3
36	6,7-dimethoxy-2-tetralone	210	(98−320)	3
42	cotinine	1500	(900−2100)	4

[a] The compounds are listed in ascending order of the IC_{50} values. [b] In Figures 1 and 2. [c] Derived from superimposition of molecules.

A series of chemicals were tested for CYP2A6 inhibitory activity, and CoMFA models were developed to understand the steric and electrostatic properties involved in the interaction. The results show that several naphthalene derivatives are potent inhibitors of CYP2A6, and minor alterations in chemical structures have a major impact on the inhibition potency. The generated CoMFA models predicted with good accuracy the inhibition potencies of several test compounds, and these models yielded clues on how to further increase potency toward the CYP2A6 enzyme. In addition, similar characteristics were determined for the homologous mouse CYP2A5 enzyme. Knowledge about CYP2A5 will aid in subsequent in vivo animal testing of the novel CYP2A6 inhibitors.

The currently studied naphthalene derivatives represent new structures of CYP2A6 inhibitors. Some of them, such as 2-bromonaphthalene and 2-fluoronaphthalene, are potent inhibitors of CYP2A6. None of these inhibitors, however, are as potent as the most potent known inhibitors of CYP2A6 such as 4,4′-dipyridyl disulfide, methoxsalen, and tranylcypromine.[17,18,20,28] The most potent CYP2A6 inhibitors in this study were the naphthalene derivatives with a halogen or a methyl group at position 2 of the naphthalene ring. In particular, a halogen atom at this position increased the inhibition potency. The known potent inhibitors of CYP2A6 enzymes are hydrophilic compounds with a hydrogen acceptor carbonyl oxygen.[16,20,27] Therefore, it is remarkable that none of the potent inhibitors found in this study include strong hydrogen acceptor atoms.

Previous studies have shown that the CYP2A6 and CYP2A5 enzymes exhibit clearly distinct substrate and inhibitor specificities.[16,18,22,33] This is not surprising, because the amino acid similarity between CYP2A6 and CYP2A5 is only 82%[39,40] and changes in very few amino acids in the CYP2A enzyme proteins profoundly affect their substrate specificities.[16,41,42] Most of the previously studied compounds, such as lactone derivatives and miconazole, inhibit more potently CYP2A5 than of CYP2A6.[16,18] Also in this study, some of the molecules, for example, cotinine and dibromo-*p*-xylol, were more than 30 times more potent inhibitors of CYP2A5 than

Table 3. Human CYP2A6 to Mouse CYP2A5 IC_{50} Ratios of the Inhibitors

inhibitor	CYP2A6/CYP2A5 IC_{50} ratio
Group 1	
2-fluoronaphthalene	0.09
2-bromonaphthalene	0.22
naphthalene	0.34
2-methylnaphthalene	0.34
1-methylisoquinoline	0.36
2-chloronaphthalene	0.45
1,2-dicloronaphthalene	0.45
Group 2	
1,3-dimethylnaphthalene	0.84
1,5-dimethylnaphthalene	0.91
1-naphthol	0.96
1,5-dichloronaphthalene	1.04
2,3-dichloronaphthalene	1.05
1,2-dimethylnaphthalene	1.08
1,7-dimethylnaphthalene	1.2
1-chloronaphthalene	1.3
1-methylnaphthalene	1.4
Group 3	
7-methyl-2-naphthaldehyde	1.6
2-naphthol	1.8
3-methylquinoline	1.9
1,2,3,6,7-pentacloronaphthalene	2.1
β-tetralone	2.2
1,7-dimethylnaphthalene	2.2
2,7-dimethylquinoline	2.2
quinaldine	2.4
2-ethylnaphthalene	2.4
2-chlorobiphenyl	2.8
1,4-dichloronaphthalene	2.9
α-tetralone	3.6
nicotine	3.8
1,6-dimethylnaphthalene	4.0
phenanthrene	4.0
3-methylisoquinoline	5.1
2,6-dimethylnaphthalene	5.9
2,6-dimethylquinoline	7.0
2,4-dimethylquinoline	7.7
4-chlorobiphenyl	8.2
6,7-dimethoxy-2-tetralone	9.2
2-methoxynaphthalene	13.4
2,7-dichloronaphthalene	22.7
dichloro-*p*-xylol	30.4
cotinine	42.8
dibromo-*p*-xylol	48.5

Table 4. Statistics of CYP2A CoMFA Model[a]

model no.	description	q^2	S_{PRESS}	n	r^2
I	CYP2A6 Gasteiger−Hückel charge	0.50	0.69	4	0.83
II	CYP2A6 MOPAC[2] AM1 charges	0.52	0.69	3	0.87
III	CYP2A6 LUMO	0.55	0.67	4	0.84
IV	CYP2A5 Gasteiger−Hückel charge	0.52	0.50	3	0.85

[a] CoMFA = model included steric and electrostatic field; LUMO = model included LUMO fields, which were calculated using MOPAC[2] AM1 method; q^2 = the crossvalidated correlation coefficient; S_{PRESS} = standard deviation for the error of prediction; n = number of PLS components, r^2 = correlation coefficient.

of CYP2A6. However, many of the studied naphthalene derivatives were more potent inhibitors of CYP2A6 than CYP2A5.

The active site of CYP2A5 is larger than that of CYP2A6.[22] Despite this, differences of inhibition potencies among compounds against CYP2A6 or CYP2A5 are likely to be due to their chemical character rather than their size.[33] The present study further strengthened this concept, because the many naphthalene derivatives are very close to each other with respect to their size and yet they exhibited widely different inhibition potencies toward CYP2A6 and CYP2A5. It can be concluded that the different amino acid residues at the active sites of CYP2A6 and CYP2A5 create unique environments, conferring on them distinct inhibition properties.

Estimations of cytochrome P450 enzyme substrate binding affinities have been made based, for example, on hydrogen bonding, $\pi-\pi$ stacking, and desolvation properties.[43−45] It is likely that lipophilicity and the number and disposition of hydrogen bond donors/acceptors within the various substrate molecules greatly affect on their enzyme selectivity and binding affinity.[43,44] In the present study, however, electrostatic interactions other than hydrogen bonding were found to account for the differences in inhibition potencies. This indicates that hydrogen bonding between the naphthalene type inhibitor and enzyme are not of major importance in the case of CYP2A6 and CYP2A5, supporting the result of our previous study.[22] In the standard CYP2A6 CoMFA models (models I and II), the significance of electrostatic interactions was not clear because the extent of partial negative charge at position 2 of the naphthalene ring did not correlate well with the inhibition potencies of compounds. In contrast, the CYP2A6 model with the LUMO fields (model III) clearly shows the dependency between electrostatic interactions and inhibition potency. In this model, a partial negative charge near naphthalene positions 1, 2, and 5 as well as a partial positive charge near position 8 increased inhibition potency. This is consistent with the CoMFA model created with lactone derivatives in our previous study.[22] Thus, the present models give more detailed information on especially the electrostatic requirements of inhibitor molecules.

The LUMO aspect of CYP2A inhibitors turned out to be significant, because the CoMFA maps with the LUMO fields show areas where changes in the fields are closely related with the inhibition potency of the inhibitors. Most probably these maps reflect charge-transfer interactions between the ligand and the binding site of the enzyme. One explanation for importance of LUMO fields describes charge transfer or $\pi-\pi$ stacking between CYP2A inhibitors and aromatic acid residues of the binding cavity. Both of these interactions are inadequately described by steric and electrostatic fields. In our previous study,[22] it was shown that $\pi-\pi$ stacking is an important interaction to orientate the molecule into correct inhibition position. We have demonstrated previously that the LUMO fields may relate to C−C double bond structures needed for binding of a ligand with the CYP2A5 protein.[21] Thus, the current CYP2A6 CoMFA maps including LUMO fields revealed novel properties required of inhibitors.

Nicotine is metabolized primarily by 5′-oxidation to form a nicotine iminium ion.[4] Previous studies have demonstrated that nicotine is orientated for oxidation at the 5′-position via a combination of hydrogen bonding and $\pi-\pi$ stacking interaction in CYP2A6.[46] In the present study, the models were improved markedly if position 5 of the pyrrolidine ring of nicotine was superimposed with position 7 of the naphthalene derivatives and pyridine nitrogen with position 3 of naphthalene derivatives. The inhibition potency of nicotine for CYP2A6 is not high, although nicotine is

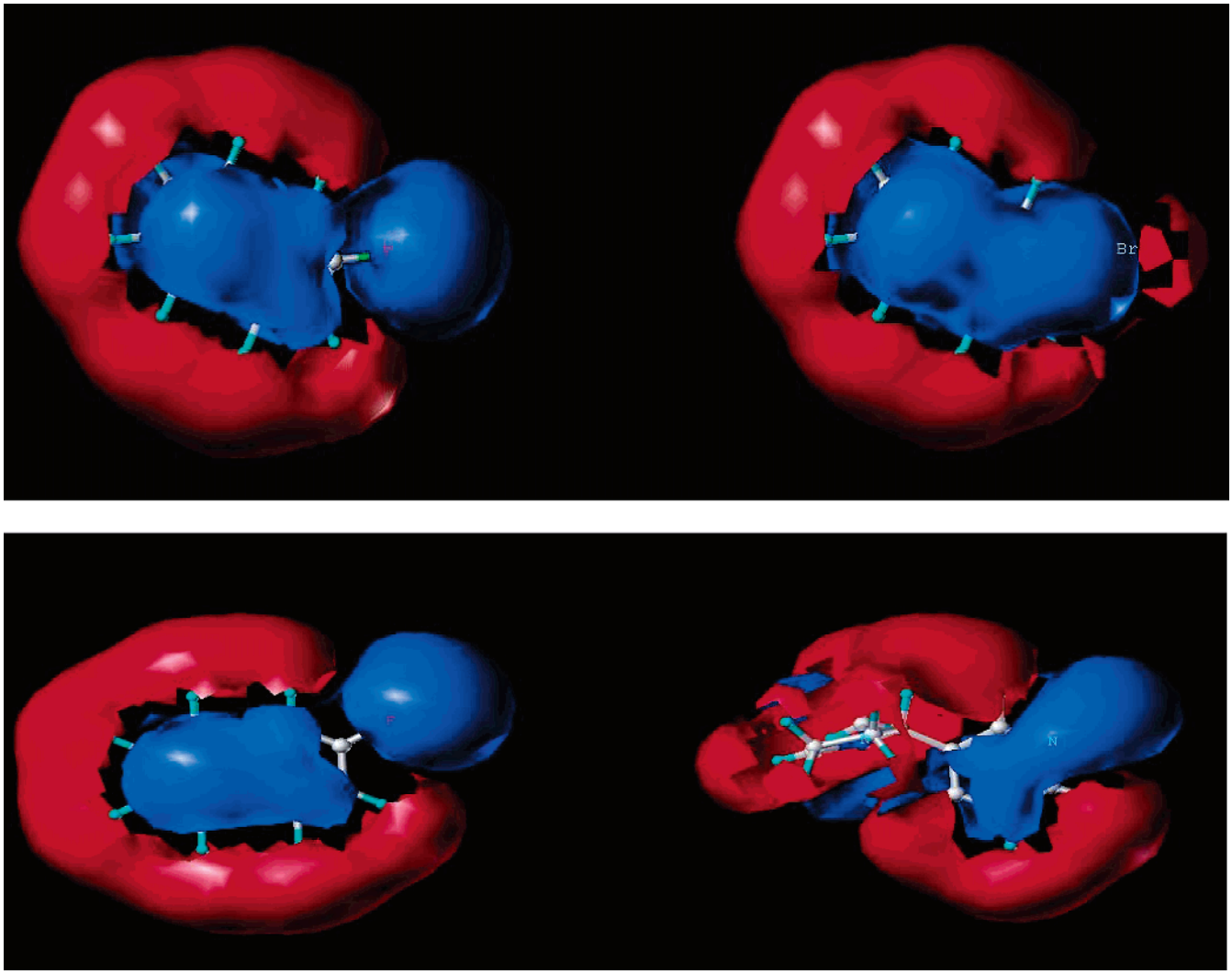

Figure 3. Superimposition of inhibitory compounds. 2-Fluoronaphthalene and 2-bromonaphthalene are examples of superimposition of compounds belonging to the same group (upper panel). 2-Fluoronaphthalene and nicotine are examples of superimposition of compound belonging to different groups (lower panel).

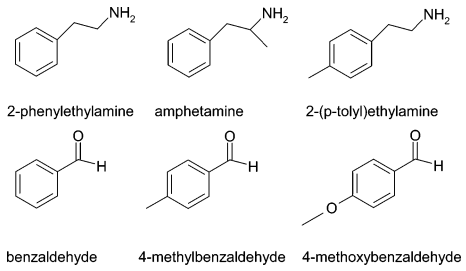

Figure 4. Structures of the inhibitors used in model validation.

mainly metabolized to cotinine by the CYP2A6 and aldehyde oxidase enzymes. In CoMFA, the low inhibition potency of nicotine is explained by the unfavorable electronegative electrostatic fields in the region superimposed on carbons 7 and 8 of the naphthalene ring.

When assessed with an external test set of compounds, both the CYP2A6 and the CYP2A5 CoMFA models (models II and IV) predicted well the pIC_{50} values of the benzaldehyde derivatives. The predicted pIC_{50} values of the CYP2A6 model for amine derivatives were also close to the experimental pIC_{50} values. This is remarkable as these molecules have one benzene ring instead of the two in the naphthalene derivatives. Obviously, steric interactions are not crucial in explaining the variations in inhibition potency of these molecules, and the generated CoMFA models explain well the variation between molecules having differences in electrostatic interactions.

In conclusion, this study describes the inhibition potencies of a series of naphthalene compounds toward the human CYP2A6 and the mouse CYP2A5 enzymes. CoMFA models were developed to obtain detailed information on structure−activity relationships on inhibitor−CYP2A enzyme interactions. These models yielded novel information of the molecular properties of CYP2A enzyme inhibitors. In addition, the models were able to accurately predict the inhibition potencies of both naphthalene and non-naphthalene derivatives. Thus, the models provide tools to test the inhibition potencies of new compounds in silico. Further refinement of the CoMFA models using larger and structurally more diverse chemical libraries is currently being done. The ultimate aim of this research is to develop potent and specific CYP2A6 inhibitors that upon coadministration with nicotine will increase its bioavailability in smoking cessation therapy.

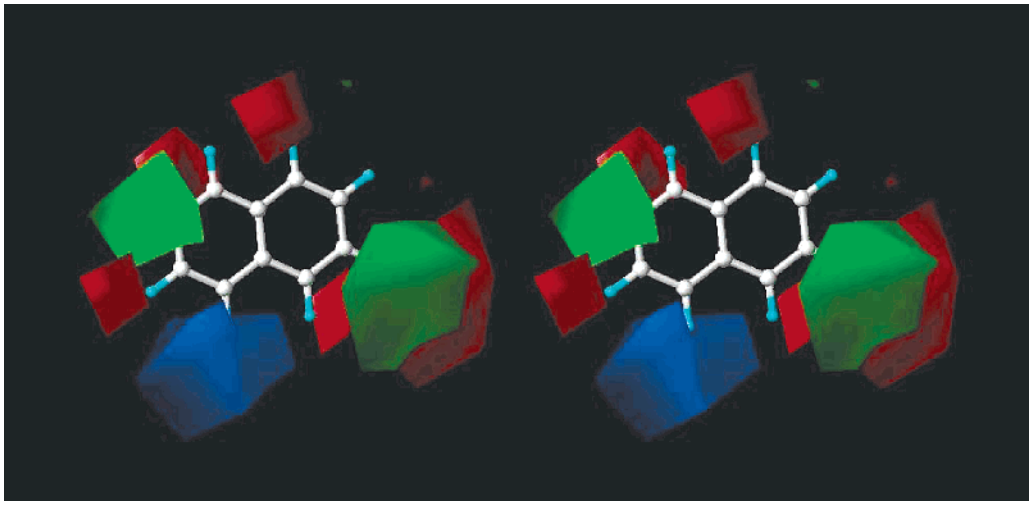

Figure 5. Stereo figure of color contour maps of CYP2A6 CoMFA with the LUMO field (model III, Table 4). Red and green represent areas where more negative partial charge and bulkier groups increase binding affinity, respectively. Blue and yellow represent areas where more negative partial charge and bulkier groups decrease binding affinity, respectively. The reference structure is 2-fluoronaphthalene.

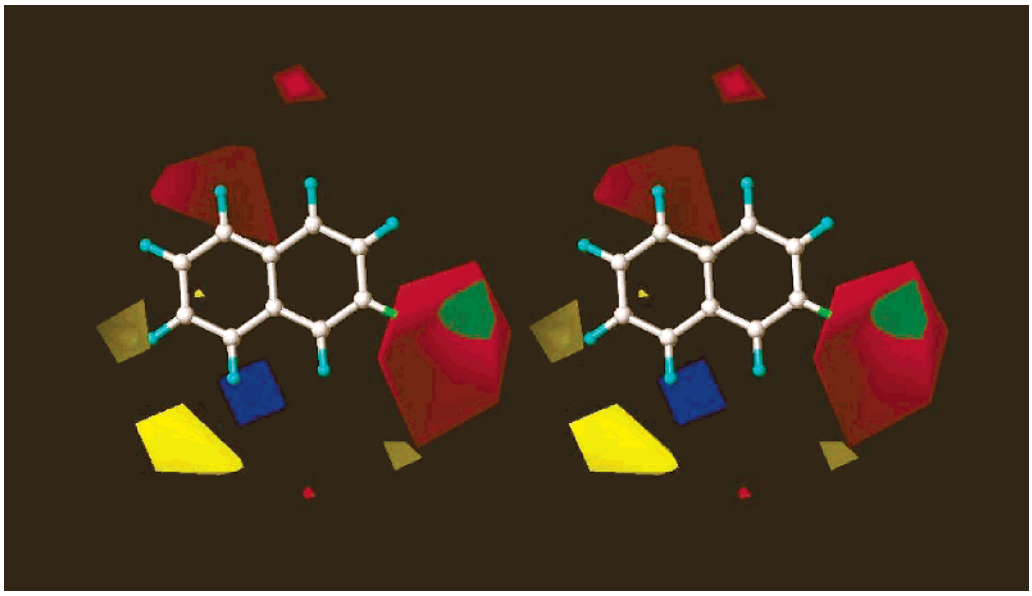

Figure 6. Stereo figure of color contour maps of CYP2A5 CoMFA with Gasteiger−Hückel charges (model IV, Table 4). See legend to Figure 5. The reference structure is 2-fluoronaphthalene.

Experimental Section

Chemicals. Naphthalene, NADPH, 1-naphthol, and 2-naphthol were purchased from Merck (Darmstadt, Germany). 1,2-Dimethylnaphthalene, 1,3-dimethylnaphthalene, 1,5-dimethylnaphthalene, 1,6-dimethylnaphthalene, 1,7-dimethylnaphthalene, 2,6-dimethylnaphthalene, 2,7-dimethylnaphthalene, 6,7-dimethoxy-2-tetralone, 2,4-dimethylquinol, 3-methylquinoline, 2,6-dimethylquinoline, 2,7-dimethylquinoline, 1-methylisoquinoline, 3-methylisoquinoline, 2-ethylnaphthalene, 1-methylnaphthalene, 2-methylnaphthalene, phenanthrene, quinaldine, α-tetralone, *β*-tetralone, dibromo-*p*-xylol, and dichloro-*p*-xylol were from Aldrich (U.S.A.). 1-Chloronaphthalene, 2-chloronaphthalene, 1,2-dichloronaphthalene, 1,4-dichloronaphthalene, 1,5-dichloronaphthalene, 2,3-dichloronaphthalene, 1,2,3,6,7-pentachloronaphthalene, 2-chlorobiphenyl, and 4-chlorobiphenyl were from Promochem (Boras, Sweden). 2-Bromonaphthalene, 2-methoxynaphthalene, 7-methyl-2-naphthaldehyde, 2,7-dichloronaphthalene, nicotine, and cotinine were from Sigma-Aldrich (St. Louis, MO). 2-Fluoronaphthalene was from Supelco (St. Louis, MO). The purity of all compounds used was higher than 95% according to the manufacturers. The compounds were dissolved in ethanol, and the final concentration of ethanol was below 2% in all incubations.

Biological Material. Male and female (7−12 weeks old; 15−25 g body weight) DBA/2N/Kuo mice were given pyrazole in saline (150 mg/kg, ip) on three consecutive mornings and killed 24 h after the last injection. Pyrazole was administered to these mice to maximize their CYP2A5 oxidizing capacity.[25] The livers were removed into ice-cold saline, combined, and pooled; microsomes were prepared as described earlier.[26] The Ethics Committee for Animal Experiments, University of Kuopio approved these experiments. Human liver samples were obtained from patients undergoing surgery to remove hepatic tumours. The patients have been described previously.[27,28] The use of surplus tissue was approved by the Ethics Committee of the University of Kuopio. Liver samples were frozen in liquid nitrogen and stored at −70 °C. Only tumor-free tissue was used for the experiments. The use of mouse and human liver microsomes as an enzyme source is justified by the fact that the coumarin 7-hydroxylation reaction is mediated exclusively by the CYP2A5 and CYP2A6 enzymes in pyrazole-treated mouse and human liver, respectively.[16,17,29−31]

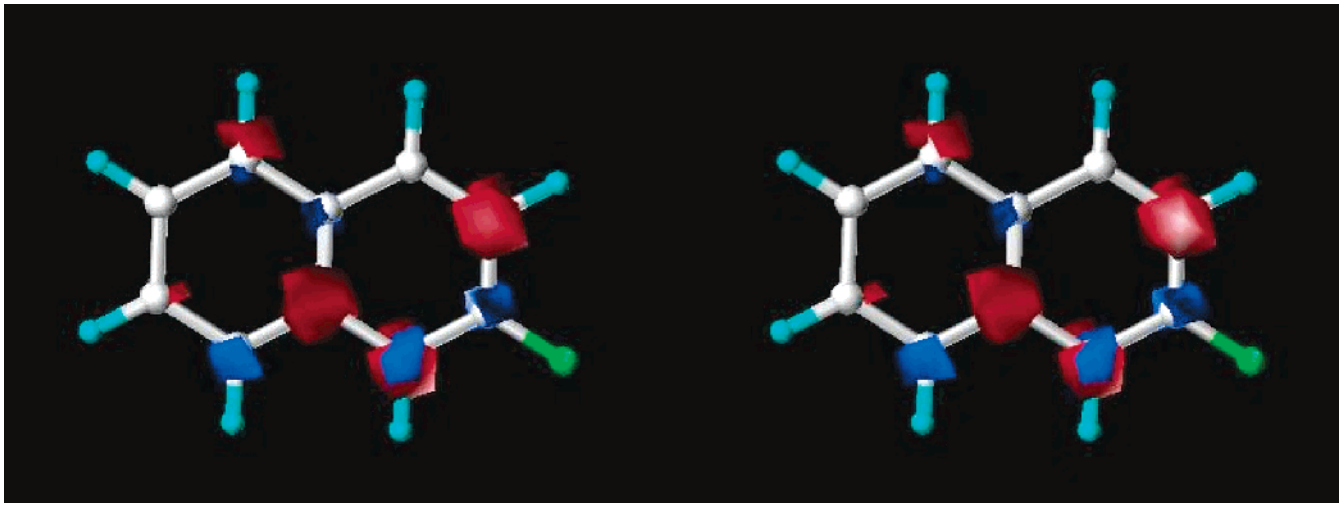

Figure 7. Stereo figure of LUMO contour map of CYP2A6 (model III, Table 4). Red areas indicate LUMO fields increase inhibition potency and blue areas indicate LUMO field decrease inhibition potency.

Table 5. Validation of the CYP2A6 and CYP2A5 Models[a]

inhibitor	pIC_{50}		
	experimental	predicted	residual
	CYP2A6		
benzaldehyde	3.92	3.81	0.11
4-methylbenzaldehyde	4.88	4.82	0.06
4-methoxybenzaldehyde	5.15	5.10	0.05
amphetamine	3.50	3.50	0
2-(*p*-tolyl)-ethylamine	5.30	5.07	0.23
2-phenylethylamine	4.41	4.50	0.09
	CYP2A5		
benzaldehyde	3.28	3.38	0.1
4-methylbenzaldehyde	4.68	4.58	0.1
4-methoxybenzaldehyde	5.23	5.33	0.1
amphetamine	2.85	3.92	1.07
2-(*p*-tolyl)-ethylamine	4.0	3.95	0.05
2-phenylethylamine	3.0	4.30	1.3

[a] The predicted pIC_{50} values were obtained from CYP2A6 CoMFA model with MOPAC AM1 charges (model II) and CYP2A5 CoMFA model with Gasteiger−Hückel charges (model IV).

Therefore, in vitro inhibition of coumarin 7-hydroxylation in mouse and human liver microsomes reflects only inhibition of CYP2A5 and CYP2A6 enzymes with no participation by other CYP forms.

Biochemical Assays. The coumarin 7-hydroxylation activity assay is based on the detection of fluorescence emitted by 7-hydroxycoumarin in alkaline conditions by spectrophotofluorometry as described by Aitio.[32] We have adapted this method to a 96-well plate format to facilitate higher throughput inhibition analysis.[33] In each well, a 100 μL incubation volume contained 50 mM Tris-HCl buffer (pH 7.4), 5.0 mM $MgCl_2$, 10 μM coumarin, 20 μg of microsomal proteins, and 0.3 mM NADPH. The reaction was initiated by addition of NADPH, incubated at 37 °C for 10 min, and terminated by adding 60 μL of 10% TCA. Immediately before the measurement, 140 μL of 1.6 M glycine-NaOH buffer (pH 10.4) was added. The formed fluorescence was measured with a Victor^2 plate counter (Perkin-Elmer Life Sciences Wallac, Turku, Finland) at 355 nm excitation and 460 nm emission. The linearity of the reaction with respect to incubation time and microsomal protein concentration was determined. Several control incubations were carried out to determine the effect of quenching by the inhibitors and other interfering factors. Each inhibitor was prescreened using inhibitor concentrations ranging from 0.1 to 1000 μM. The actual IC_{50} values were determined using narrower inhibitor concentration ranges with five to seven concentrations. All IC_{50} values were determined in duplicate from two different human liver microsomal preparations or pooled mouse liver microsomal samples.

The solubility of most inhibitors did not cause problems in the determination of inhibition potency. However, the lipophilicity of dichloroxylol, dibromoxylol, 1,2-dichloronaphthalene, 2,3-dichloronaphthalene, phenanthrene, and 1,2,3,6,7-pentachloronaphthalene was so high that the IC_{50} values of these molecules could not be determined at the 10 μM substrate concentration. In these cases, 1 μM coumarin was used, and the IC_{50} values were calculated using the equations $K_I = I/(v_0/v - 1)(1 + S/K_m)$ [34] and $IC_{50} = K_I + (K_I/K_m)S$,[35] using $S = 1$ μM coumarin, $K_m = 0.64$ μM for CYP2A5 and $K_m = 0.74$ for CYP2A6.[19] IC_{50} values were calculated using nonlinear regression analysis with Prism 3.0 software (San Diego, CA).

Because the purpose of this study was to create models for CYP2A6/5 enzymes inhibition, IC_{50} values (measuring relative inhibition potency) rather than the absolute K_i values were determined. This is justified because all measurements were made in standardized conditions and the results are thus fully comparable with each other. The validation of the models was carried out with compounds that were measured exactly as those used in the models.

CoMFA Models. The structure−activity relationships of the molecules were analyzed using the CoMFA method.[36] Construction of the molecules, superimposition, and CoMFA modeling were performed using Sybyl 6.9 (TRIPOS Associates Inc., St. Louis, MO) molecular modeling software. Molecules were created using the sketch option in Sybyl. The conformation of any side chains was fully performed by systematic search option. The biological data was transformed to pIC_{50} values. Three CoMFA models were created for CYP2A6 enzymes and one for CYP2A5. All analyses contained steric and electrostatic fields, which were calculated using the Tripos force field[37] with an sp^3-hybridized carbon (charge +1) as a probe atom with a 2 Å grid spacing. The standard CoMFA models for the CYP2A6 enzymes were created using either Gasteiger−Hückel atomic point charges (model I) or MOPAC AM1 charges (model II). The CYP2A5 CoMFA model (model IV) was created using Gasteiger−Hückel atomic point charges.[38] The standard deviation threshold for exclusion of columns from the PLS analysis was set at 1 kcal/mol. The third CYP2A6 CoMFA model (model III) included steric and electrostatic fields with the LUMO field. The region for the LUMO field was created using 2-fluoronaphthalene as the model molecule, and the threshold value was set at 0.001. In the CoMFA analyses including LUMO fields, the structures, atomic point charges, and wavefunctions for each molecule were calculated using the MOPAC program with AM1 parametrization.[38] The PLS method with five random group cross validation was used for statistical analyses, and this calculation was repeated 20 times to verify the stability of the model. The optimum number

of components for the nonvalidated analyses was chosen using the lowest S_{PRESS} value and the highest q^2 value.

Molecules were superimposed by root-mean-squares (rms) fit based on their structures and inhibition potencies. The inhibitors were stratified into several groups according to their inhibition potencies. Inhibitors belonging in the same group were superimposed by manually increasing electrostatic field similarity (Tables 1 and 2, Figure 3a). Within each group, the superimposition of the electrostatic fields was similar. For example, 2-fluoronaphthalene and 2-bromonaphthalene belong to the same superimposition group because their CYP2A6 IC_{50} values were close to each other. Inhibitors that had large differences in their IC_{50} values, such as nicotine and 2-fluoronaphthalene, exhibited also distinct electrostatic fields and consequently were superimposed in a different manner (Tables 1 and 2, Figure 3b).

An external test set of chemicals (Figure 4) was used to estimate the predictability of the generated CoMFA models. The biological data (pIC_{50} values) of the test set molecules were obtained from our previous work.[33]

Acknowledgment. The authors thank Virpi Koponen for excellent technical help and Dr. Ewen MacDonald, MSc (Phar.) Laura Kornonen, MSc (Phar.) Outi Salo, and MSc Toni Rönkkö for comments during the work. The work was funded by the Finnish National Technology Agency TEKES (80002/02).

References

(1) Khurana, S.; Batra, V.; Patkar, A. A.; Leone, F. T. Twenty-First Century Tobacco Use: It is not Just a Risk Factor Anymore. *Respir. Med.* **2003**, *97*, 295−301.
(2) World Health Organization. *The World Health Report 2002: Reducing Risks, Promoting Healthy Life*; World Health Organization: Geneva, 2002.
(3) Ezzati, M.; Vander Hoorn, S.; Rodgers, A.; Lopez, A. D.; Mathers, C. D.; Murray, C. J. L. Estimates of Global and Regional Potential Health Gains from Reducing Multiple Major Risk Factors. *Lancet* **2003**, *362*, 271−280.
(4) Benowitz, N. L. Pharmacology of Nicotine: Addiction and Therapeutics. *Annu. Rev. Pharmacol. Toxicol.* **1996**, *36*, 597−613.
(5) Oscarson, M. Genetic Polymorphisms in the Cytochrome P450 2A6 (CYP2A6) Gene: Implications for Interindividual Differences in Nicotine Metabolism. *Drug Metab. Dispos.* **2001**, *29*, 91−95.
(6) Raunio, H.; Rautio, A.; Gulstenn, H.; Pelkonen, O. Polymorphisms of CYP2A6 and its Practical Consequences. *Br. J Clin. Pharmacol.* **2001**, *52*, 357−363.
(7) Sellers, E. M.; Tyndale, R. F.; Fernandes, L. C. Decreasing Smoking Behaviour and Risk Through CYP2A6 Inhibition. *Drug Discovery Today* **2003**, *8*, 487−493.
(8) Kitagawa, K.; Kunugita, N.; Katoh, T.; Yang M.; Kawamoto, T. The Significance of the Homozygous CYP2A6 Deletion on Nicotine Metabolism: a New Genotyping Method of CYP2A6 Using a Single PCR−RFLP. *Biochem. Biophys. Res. Commun.* **1999**, *262*, 146−151.
(9) Inoue, K.; Yamazaki, H.; Shimada, T. CYP2A6 Genetic Polymorphisms and Liver Microsomal Coumarin and Nicotine Oxidation Activities in Japanese and Caucasians. *Arch. Toxicol.* **2000**, *73*, 532−539.
(10) Nakajima, M.; Yamagishi, S. I.; Yamamoto, H.; Yamamoto, T.; Kuroiwa, Y.; Yokoi, T. Deficient Cotinine Formation from Nicotine is Attributed to the Whole Deletion of the CYP2A6 Gene in Humans. *Clin. Pharmacol. Ther.* **2000**, *67*, 57−69.
(11) Tyndale, R. F.; Sellers, E.; M. Genetic Variation in CYP2A6 mediated Nicotine Metabolism Alters Smoking Behavior. *Ther. Drug Monit.* **2002**, *24*, 163−171.
(12) Sellers, E. M.; Kaplan, H. L.; Tyndale, R. F. Inhibition of Cytochrome P450 2A6 Increases Nicotine's oral Bioavailability and Decreases Smoking. *Clin. Pharmacol. Ther.* **2000**, *68*, 35−43.
(13) Tyndale, R. F.; Sellers, E. M. Variable CYP2A6 Mediated Nicotine Metabolism Alters Smoking Behavior and Risk. *Drug Metab. Dispos.* **2001**, *29*, 548−552.
(14) Takeuchi, H.; Saoo, K.; Yokohira, M.; Ikeda, M.; Maeta, H.; Miyazaki M.; Yamazaki H.; Kamataki, T.; Imaida, K. Pretreatment with 8-Methoxypsoralen, a Potent Human CYP2A6 Inhibitor, Strongly Inhibits Lung Tumorigenesis Induced by 4-(Methylnitrosamino)-1-(3-Pyridyl)-1-Butanone in Female A7J Mice. *Cancer Res.* **2003**, *63*, 7581−7583.
(15) Miyamoto, M.; Umetsu, Y.; Dosaka-Akita, H.; Sawamura, Y.; Yokota, J.; Kunitoh, H.; Nemoto, N.; Sato, K.; Ariyoshi Kamataki, T. CYP2A6 Gene Deletion Reduces Susceptibility to Lung Cancer. *Biochem. Biophys. Res. Commun.* **1999**, *261*, 658−660.
(16) Juvonen, R. O.; Gynther, J.; Pasanen, M.; Alhava, E.; Poso, A. Pronounced Differences in Inhibition Potency of Lactone and Non-lactone Compounds for Mouse and Human Coumarin 7-Hydroxylases (CYP2A5 and CYP2A6). *Xenobiotica* **2000**, *30*, 81−92.
(17) Draper, A. J.; Madan, A.; Parkinson, A. Inhibition of Coumarin 7-Hydroxylase Activity in Human Liver Microsomes. *Arch. Biochem. Biophys.* **1997**, *341*, 47−61.
(18) Mäenpää, J.; Sigushi, H.; Raunio, H.; Syngelma, T.; Vuorela, P.; Vuorela, H.; Pelkonen, O. Differential Inhibition of Coumarin 7-Hydroxylase Activity in Mouse and Human Liver Microsomes. *Biochem. Pharmacol.* **1993**, *45*, 1035−1042.
(19) Kimonen, T.; Pasanen, M.; Gynther, J.; Poso, A.; Järvinen, T.; Alhava, E.; Juvonen, R. O. Competitive Inhibition of Coumarin 7-Hydroxylation by Pilocarpine and Its Interaction with Mouse CYP 2A5 and human CYP 2A6. *Br. J. Pharmacol.* **1995**, *116*, 2652−2630.
(20) Fujita, K.; Kamataki, T. Screening of Organosulfur Compounds as Inhibitors of Human CYP2A6. *Drug Metab. Dispos.* **2001**, *29*, 983−989.
(21) Poso, A.; Juvonen, R.; Gynther, J. Comparative Molecular Field Analysis of Compounds with CYP2A5 Binding Affinity. *Quant. Struct.−Act. Relat.* **1995**, *14*, 507−511.
(22) Poso, A.; Gynther, J.; Juvonen, R. A Comparative Molecular Field Analysis of Cytochrome P450 2A5 and 2A6 Inhibitors. *J. Comput.-Aided Mol. Des* **2001**, *15*, 195−202.
(23) Lewis, D. F.; Dickins, M.; Lake, B. G.; Eddershaw, P. J.; Tarbit, M. H.; Goldfarb, P. S. Molecular Modelling of the Human Cytochrome P450 Isoform CYP2A6 and Investigations of CYP2A Substrate Selectivity. *Toxicology* **1999**, *133*, 1−33.
(24) Asikainen, A.; Tarhanen, J.; Poso, A.; Pasanen, M.; Alhava, E.; Juvonen, R. O. Predictive Value of Comparative Molecular Field Analysis Modelling of Naphthalene Inhibition of Human CYP2A6 and Mouse CYP2A5 Enzymes. *Toxicol. in Vitro* **2003**, *17*, 449−455.
(25) Juvonen, R.; Kaipainen, P. K.; Lang, M. A. Selective Induction of Coumarin 7-Hydroxylase by Pyrazole in D2 mice. *Eur. J. Biochem.* **1985**, *152*, 3−8.
(26) Lang, M. A.; Nebert, D. W. Structural Gene Products of the Ah Locus. Evidence for Many Unique P-450-mediated Monooxygenase Activities Reconstituted from 3-Methylcholanthrene-Treated C57BL/6N Mouse Liver Microsomes. *J. Biol. Chem.* **1981**, *256*, 12058−12067.
(27) Kimonen, T.; Juvonen, R. O.; Alhava, E.; Pasanen, M. The Inhibition of CYP Enzymes in Mouse and Human Liver by Pilocarpine. *Br. J. Pharmacol.* **1995**, *114*, 832−836.
(28) Taavitsainen, P.; Juvonen, R.; Pelkonen, O. In Vitro Inhibition of Cytochrome P450 Enzymes in Human Liver Microsomes by a Potent CYP2A6 Inhibitor, Trans-2-phenylcyclopropylamine (tranylcypromine), and its Nonamine Analog, Cyclopropylbenzene. *Drug Metab. Dispos.* **2001**, *29*, 217−222.
(29) Chang, T. K.H.; Waxman, D. J. The CYP2A Subfamily. In *Cytochromes P450 Metabolic and Toxicological Aspects*; Ionnides, C., Ed.; CRC Press: Boca Raton, 1996; pp 99−134.
(30) Pelkonen, O.; Raunio, H.; Rautio, A.; Pasanen, M.; Lang, M. A. The Metabolism of Coumarin. In *Coumarins: Biology, Applications and Mode of Action*; O'Kennedy, R., Thornes, R. D., Eds.; John Wiley & Sons Ltd: Chichester; New York 1997; pp 67−92.
(31) Pelkonen, O.; Rautio, A.; Raunio, H.; Pasanen, M. CYP2A6: a Human Coumarin 7-Hydroxylase. *Toxicology* **2000**, *144*, 139−147.
(32) Aitio, A. A Simple and Sensitive Assay of 7-Ethoxycoumarin Deethylation. *Anal. Biochem.* **1978**, *85*, 488−491.
(33) Rahnasto, M.; Raunio, H.; Poso, A.; Juvonen, R. O. More Potent Inhibition of Human CYP2A6 than Mouse CYP2A5 Enzyme Activities by Derivatives of Phenylethylamine and Benzaldehyde. *Xenobiotica* **2003**, *33*, 529−539.
(34) Torneheim, K. Kinetic Applications Using High Substrate and Competitive Inhibitor Concentrations to Determine K_i or K_m. *Anal. Biochem.* **1994**, *221*, 53−56.
(35) Venalainen, J. I.; Juvonen, R. O.; Forsberg, G. M. M.; Garcia-Horsman, A.; Poso, A.; Wallen, E. A.; Gynther, J.; Mannisto, P. T. Substrate-Dependent, Non-Hyperbolic Kinetics of Pig Brain Prolyl Oligopeptidase and its Tight Binding Inhibition by JTP-4819. *Biochem. Pharmacol.* **2002**, *64*, 463−471.
(36) Cramer, R. D.; Patterson, D. E., III; Bunce, J. D. Comparative Molecular Field Analysis (CoMFA). 1. Effect of Shape on Binding of Steroids to Carrier Proteins. *J. Am. Chem. Soc.* **1988**, *110*, 5959−5967.

(37) Clark, M.; Cramer, R. D. I.; Van Opdenbosch, N. Validation of the General Purpose Tripos 5.2 Force Field. *J. Comput. Chem.* **1989**, *10*, 982−1012.
(38) Dewar, M. J. S.; Zoebisch, E. G.; Healy, E. F.; Stewart, J. J. P. AM1: a New General Purpose Quantum Mechanical Molecular Model. *J. Am. Chem. Soc.* **1993**, *115*, 8.
(39) Miles, J. S.; Mclaren, A. W.; Forrester, L. M.; Glancey, M. J.; Lang, M. A.; Wolf, C. R. Identification of the Human Liver Cytochrome P-450 Responsible for Coumarin 7-Hydroxylase Activity. *Biochem. J.* **1990**, *267*, 365−371.
(40) Yamano, S.; Tatsuno, J.; Gonzales, F. J. The CYP2A3 Gene Product Catalyzes Coumarin 7-Hydroxylation in Human Liver Microsomes. *Biochemistry* **1990**, *29*, 1322−1329.
(41) Lindberg, R. L. P.; Negishi, M. Alteration of Mouse Cytochrome $P450_{coh}$ Substrate Specificity by Mutation of a Single Amino-Acid Residue. *Nature* **1989**, *339*, 632−634.
(42) Lewis, D. F.; Lake, B. G. Species Differences in Coumarin Metabolism: a Molecular Modelling Evaluation of CYP2A Interactions. *Xenobiotica* **2002**, *32*, 547−561.
(43) Lewis, D. F. V.; Dickins, M. Substrate SARs in Human P450s. *Drug Discovery Today* **2002**, *7*, 918−925.
(44) Lewis, D. F. V. Essential Requirements for Substrate Binding Affinity and Selectivity Toward Human CYP2 Family Enzymes. *Arch. Biochem. Biophys.* **2003**, *409*, 32−44.
(45) Lewis, D. F. V.; Modi, S.; Dickins, M. Structure−Activity Relationship for Human Cytochrome P450 Substrates and Inhibitors. *Drug Metab. Rev.* **2002**, *34*, 69−82.
(46) Lewis, D. F. V.; Gorrod, J. W. Molecular Orbital Calculations and Nicotine Metabolism: a Rationale for Experimentally Observes Metabolite Ratios. *Drug Metab. Drug Interact.* **2002**, *19*, 29−39.

JM049536B